OPEN

Journal of Cerebral Blood Flow & Metabolism (2014) 34, 1117–1127

www.jcbfm.com

ORIGINAL ARTICLE

Detecting tissue deterioration after brain injury: regional blood flow level versus capacity to raise blood flow

Delphine Feuerstein[1,4], Masatoshi Takagaki[1,4], Markus Gramer[1], Andrew Manning[2], Heike Endepols[1], Stefan Vollmar[1], Toshiki Yoshimine[3], Antony J Strong[2], Rudolf Graf[1,4] and Heiko Backes[1,4]

Regional cerebral blood flow (*rCBF*) is spatially and temporally adjusted to local energy needs. This coupling involves dilation of vessels both at the site of metabolite exchange and upstream of the activated region. Deficits in upstream blood supply limit the 'capacity to raise *rCBF*' in response to functional activation and therefore compromise brain function. We here demonstrate in rats that the 'capacity to raise *rCBF*' can be determined from real-time measurements of *rCBF* using laser speckle imaging during an energy challenge induced by cortical spreading depolarizations (CSDs). Cortical spreading depolarizations (CSDs) occur with high incidence in stroke and various other brain injuries and cause large metabolic changes. Various conditions of cerebral perfusion were induced, either by modifying microvascular tone, or by altering upstream blood supply independently. The increase in *rCBF* per unit of time in response to CSD was linearly correlated to the upstream blood supply. In an experimental model of stroke, we found that this marker of the capacity to raise *rCBF* which, in pathologic tissue may be additionally limited by impaired vasoactive signaling, was a better indicator of the functional status of cerebral tissue than local *rCBF* levels.

Journal of Cerebral Blood Flow & Metabolism (2014) **34,** 1117–1127; doi:10.1038/jcbfm.2014.53; published online 2 April 2014

Keywords: cortical spreading depolarization; focal cerebral ischemia; upstream blood supply

INTRODUCTION

Brain activity and viability rely critically on the continuous delivery of energy substrates and oxygen via blood. During functional activation, regional cerebral blood flow (*rCBF*) is locally adjusted to meet increased energy demand by regulation of the local microvessel diameter and concomitant dilatation of upstream arterioles and arteries that supply blood to the local capillary bed. This process is commonly known as neurovascular coupling and results in *rCBF* changes that are temporally and spatially linked to neuronal activity.[1] Upstream blood supply sets the limit to the capacity of tissue to raise *rCBF* in response to functional activation and increased energy demand. Hence, any reduction in blood supply reduces tissue functionality and may result in severe cerebral damage. The term upstream blood supply should not be comprehended in an anatomic sense but rather as a functional or mechanistic concept. Upstream includes all branches of the arterial tree the blood flows through before reaching the location of metabolite exchange (glucose, O_2/CO_2) with the tissue. Under pathologic conditions, the location that limits upstream blood supply is anatomically ill defined: it can be very close to the 'exchange point' (at the level of arterioles or pial arteries in case of focal ischemia) or very far (cardiac arrest) or somewhere in between (at the site of the carotid artery for example). In any case, it is upstream of the 'exchange point' (see explanatory sketch in Supplementary Figure S6). As reductions of upstream blood supply can be partially compensated by local vessel dilation, *rCBF* levels may appear normal despite severe problems in upstream blood supply. Identification of deficits in upstream blood supply, and therefore of local functional status, could improve diagnosis and treatment of these diseases.

In the present work, we addressed the relation between local *rCBF*, microvascular tone and upstream blood supply in (1) physiologic conditions and (2) after global ischemia in rats. Regional cerebral blood flow was measured with high spatial and temporal resolution by laser speckle imaging (LSI). First, *rCBF* was modified by altering microvascular tone using two anesthetics: propofol and isoflurane. Propofol is known for reducing *rCBF* compared with other anesthetics whereas isoflurane is a volatile agent with vasodilating effects.[2] Second, in separate experiments, upstream blood supply to the brain was impeded by sequentially ligating one, then two common carotid arteries (CCAs) under isoflurane.

To induce changes in local energy demand, we elicited cortical spreading depolarizations (CSD). A CSD is a self-propagating wave of tissue depolarization that causes massive transient disruption of ion homeostasis and membrane potentials associated with significant changes in metabolism and blood flow.[3–6] Cortical spreading depolarizations can be induced mechanically or chemically in the normal brain and they spontaneously arise after brain injury, as observed experimentally[7–9] and clinically.[10–13] As such, CSD was a suitable phenomenon to investigate the *rCBF* response to an energy challenge in the healthy and in the injured brain, i.e., in conditions of normal or reduced upstream blood supply. We applied our findings in an experimental model of stroke and in two patients suffering from severe brain injury.

[1]Max Planck Institute for Neurological Research, Cologne, Germany; [2]Department of Clinical Neuroscience, Institute of Psychiatry, King's College London, London, UK and [3]Department of Neurosurgery, Osaka University Graduate School of Medicine, Osaka, Japan. Correspondence: Dr D Feuerstein, Max Planck Institute for Neurological Research, Gleueler Strasse 50, Cologne 50931, Germany.
E-mail: delphfeuerstein@gmail.com
This work was supported by the Humboldt Foundation (fellowship for postdoctoral researchers) to DF.
[4]These authors contributed equally to this work.
Received 15 October 2013; revised 27 February 2014; accepted 28 February 2014; published online 2 April 2014

MATERIALS AND METHODS

Surgical Preparation and Physiologic Monitoring in Rats

All animal procedures were performed in accordance with the German regulations for animal protection (TierSchG, 2006) and were approved by the local animal care committee and local governmental authorities (LANUV NRW) and written up following the ARRIVE guidelines. In male Wistar rats (Janvier, France; weight: 240 to 420 g; age 7 to 12 weeks; housed with an inverse 12 hours day–night cycle with lights on at 8:30 pm in a temperature ($22 \pm 1^{\circ}C$) and humidity ($55 \pm 5\%$) controlled room pairwise in type-4 cages filled with Lignocel; experiments performed between 9 am and 4 pm) general anesthesia was induced with 5% isoflurane and maintained with 2% isoflurane in 70%/30% nitrous oxide/oxygen during surgical procedures. The animals breathed spontaneously via a snout mask. Rectal temperature was kept at $37^{\circ}C$ using a servo-controlled heating blanket. The left femoral artery was cannulated for continuous monitoring of arterial blood pressure and for hourly measurement of blood gases (arterial PaO_2, $PaCO_2$, pH). In all experimental groups (see details below), the frontal and parietal bones were exposed and thinned out to transparency using a dental drill. Drilling was performed under continuous saline irrigation to prevent heat injury. The cavity formed yielded a field of view for LSI through thin skull of 12×7 mm. This field of view was symmetrical around midline for experimental groups 1 to 3 (Figure 1A) while only the left hemisphere was thinned out in experimental group 4 to provide a field of view that covered most of the cortical territory of the MCA (Figure 5A). At the end of surgery, the thinned out skull surface was covered with warm paraffin oil and laser speckle images were continuously acquired during the whole duration of the experiments.

Experimental Groups and Protocols

Group 1: Single cortical spreading depolarization under different anesthesia regimens. In five animals, after completion of skull thinning, a small burr hole was drilled into the frontal bone for subsequent needle pricks (Figure 1A). After laser speckle baseline imaging under continued isoflurane anesthesia, a single CSD wave was induced by a needle prick. Laser speckle imaging monitored the *rCBF* response for 60 minutes. Propofol infusion was then started at 38 mg/kg per hour via tail vein and isoflurane weaned off over 15 minutes. Propofol concentration (33 to 53 mg/kg per hour) was adjusted to keep breathing rate within 60 to 100 cycles per minute. Thirty minutes after isoflurane was completely off, systemic variables and *rCBF* had stabilized (Table 1). A second needle prick induced a single CSD wave again and the corresponding *rCBF* response measured for 60 minutes. In one animal, the order of the anesthesia regimens was reversed, i.e., the first needle prick was performed under propofol anesthesia and the second needle prick under isoflurane (30 minutes after propofol infusion was completely off).

Group 2: Multiple cortical spreading depolarization under different anesthesia regimens. Nine rats were divided into two subgroups according to the anesthesia regimens after surgery: either isoflurane ($n = 5$) or propofol ($n = 4$). After baseline imaging, multiple CSDs were elicited under each respective anesthesia by epidural application of a cotton ball soaked in 3 mol/L potassium chloride (KCl) solution on the frontal cortex. The cotton ball was continuously infused with KCl solution at 10 μL/hour for 30 minutes and the *rCBF* responses to multiple CSDs examined by LSI.

Group 3: Common carotid artery ligation group. In five animals, 4-0 sutures were placed loosely around each common carotid artery (CCA). A durectomy for needle prick was prepared (see above). The animals were maintained at 1.5% to 2% isoflurane and LSI was acquired during the whole experiment. After baseline imaging, a first CSD was elicited by needle prick and observed for 60 minutes. The left CCA was then ligated using the prepared suture. A drop in *rCBF* was observed in the left hemisphere, indicating successful ligation. After stabilization of blood pressure and *rCBF* (within around 15 minutes) and exclusion of spontaneously arising CSD waves, a second CSD was elicited by needle prick. Sixty minutes later, the right CCA was additionally ligated, leading to a global hypoperfusion of the whole brain. Once systemic variables and *rCBF* reached steady values, a third CSD was elicited by needle prick. Imaging continued for 60 minutes. In one animal, a spontaneous CSD propagated after the ligation of the second CCA. Hence, no third needle prick was performed in this case, and the spontaneous CSD was excluded from further analysis.

Group 4: Middle cerebral artery occlusion group. In nine rats, focal ischemia was induced by embolic occlusion of the middle cerebral artery (MCAo) using the macrosphere model described elsewhere.[7] In two rats, isoflurane anesthesia was maintained and in seven rats, anesthesia was changed to propofol (the switch from isoflurane to propofol lasted 45 minutes, 15 minutes to slowly wean isoflurane off, and 30 minutes to allow the animals to stabilize under propofol-only anesthesia). After subsequent baseline imaging for 5 minutes, the macrosphere was advanced into the intracarotid artery by injection of ~ 0.2 mL heparinized saline. This resulted in the occlusion of the MCA, and *rCBF* changes in the MCA territory were observed for up to 3 hours after macrosphere injection. The position of the macrosphere in the neurovasculature was verified postmortem by visual inspection of the base of the brain (Figure 5B).

Laser Speckle Imaging

Instrumentation and acquisition. The LSI method was implemented as previously described.[14,15] In brief, the exposed cortex was illuminated through thin skull and intact dura mater by a laser diode (DL7140-201, 785 nm, 70 mW, Sanyo Electric, Tokyo, Japan). The scattered light source produced a speckle pattern that was recorded by a CCD camera (A602f-2 Basler, Ahrensburg, Germany) using custom-written software (Andrew Dunn, University of Texas at Austin). For one single speckle contrast image, 30 consecutive raw speckle frames were acquired at 30 Hz, processed by computing the spatial speckle contrast using a sliding window of 7×7 pixels and averaged to improve the signal–to-noise ratio. Sequenced laser speckle images were thus obtained every second. Laser speckle imaging started after surgical procedures and continued uninterrupted throughout all experiments.

Region of interest analysis of dynamic cerebral blood flow. Speckle contrast images were analyzed using VINCI imaging software (Volume Imaging in Neurological Research, Max Planck Institute for Neurological Research, Cologne, Germany) and MATLAB (R2011a, Mathworks, Natick, MA, USA). Regions of interest (ROI) of 1 mm diameter were placed in areas devoid of major blood vessels (Figure 1A). For each ROI, the mean spatial speckle contrast value was converted to an inverse correlation time (ICT) value using a look-up table derived previously.[14] This yielded local time courses of ICT values that were sampled at 1 Hz over the whole duration of the experiments. Time zero was defined as the CSD induction time, i.e., time of the needle prick (groups 1 and 3) or of KCl cotton ball application (group 2) or of MCA occlusion (group 4).

Although ICT values are not equivalent to absolute measurements of *rCBF*, they do provide a good estimation of the true magnitude of cerebral blood flow changes, as demonstrated in previous validation studies.[14,16] In order to demonstrate the resulting differences in data interpretation, we used two different methods to express *rCBF* in this report:

i Regional cerebral blood flow was given by the ICT values derived from LSI. As ICT values are not direct CBF values in ml/minute per 100 g, we set the average ICT value at resting-state isoflurane ($ICT = 15.0 \pm 2.9$/millisecond) to 100% *rCBF* (resting-state isoflurane was a common condition for all animals). Accordingly, the resting-state propofol ICT value was 7.4 ± 1.1/millisecond, corresponding to 49.3% *rCBF* (Figures 1C, 1D, 2, 4C, and 5C).
ii Relative changes in *rCBF* in response to individual CSD, i.e., $\Delta rCBF$ (Figure 1B and 1E only) were given by the changes in ICT values compared with each pre-CSD ICT value taken as $\Delta rCBF = 0\%$, irrespective of the anesthesia regimens (Figure 1E, point 'base').

Arterial diameter measurement. To assess pial arterial diameter, LSI was performed through the objective of a microscope with a magnification of $\times 10$, in one animal from group 1 and in one animal from group 3.

For increased spatial resolution, temporal speckle contrast images were calculated over 40 seconds for each condition.[17] Blood vessels were automatically detected using the smallest eigenvector output of the FeatureJ Hessian plugin of ImageJ[18,19] combined with an automatic threshold selection based on the derivative of its histogram. This resulted in binary images with only the detected blood vessels. Three ROIs were positioned on separate segments along the MCA (Figures 4A and 4B) and the number of vessel pixels in each ROI was counted. This number was proportional to the vessel diameter in each ROI. Using the same ROIs for each condition, changes in arterial diameters could be determined relative to the arterial diameters under isoflurane (Figures 4C and 4D).

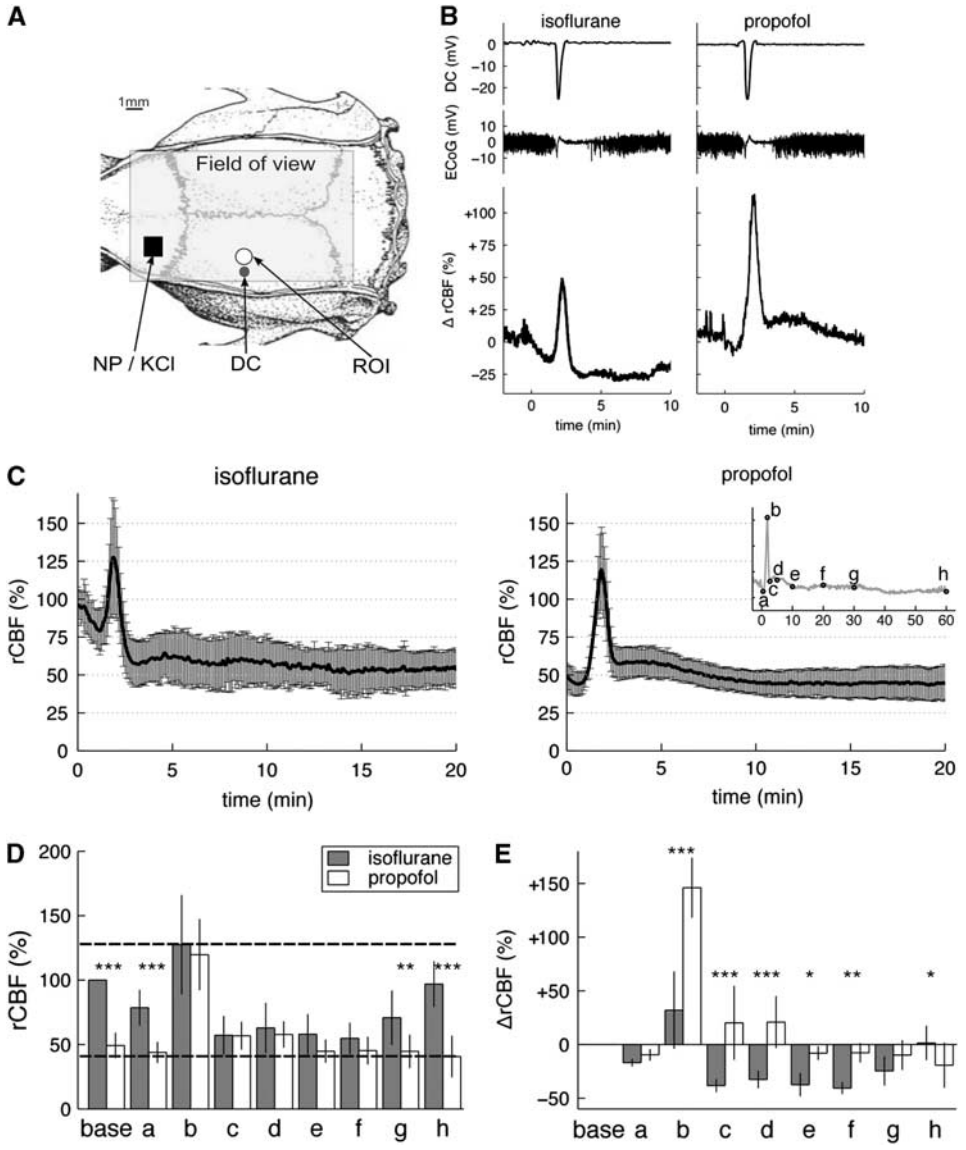

Figure 1. Regional cerebral blood flow (*rCBF*) responses to induced cortical spreading depolarizations (CSDs) under isoflurane or propofol. (**A**) Experimental setup. The field of view for laser speckle imaging (LSI) was $\sim 12 \times 7$ mm. Cortical spreading depolarizations were induced either by needle prick (NP) or epidural 3 mol/L KCl application in the frontal lobe (black square). A circular region of interest (ROI) of 1 mm diameter was placed 5 mm posterior to the CSD induction site. This ROI was analyzed for *rCBF* in groups 1 to 3. A direct current (DC) microelectrode (black circle marked DC) was implanted ~ 5 mm posterior to the CSD induction site and 4 mm lateral to midline. (**B**) Representative electrophysiological (top traces) and relative $\Delta rCBF$ responses (bottom trace) to a single CSD wave induced alternatively under isoflurane (left) and under propofol (right) anesthesia in the same animal (experimental group 1). Time $t = 0$ was the time of the NP. Baseline DC potential and baseline $\Delta rCBF$ were taken as the average value over 2 minutes before each NP and set to 0. (**C**) Average time courses of the *rCBF* responses to a single CSD in five animals under isoflurane (left) and propofol (right) shown as mean $\pm$ s.d. (error bars). The *rCBF* 100% value was given as the average value over 2 minutes before NP under isoflurane anesthesia. (**D**) Bar plots of the *rCBF* values under isoflurane anesthesia (dark gray bars) and propofol anesthesia (white bars) at characteristic time points (a to h) defined as per insert in (**C**). Point 'base' refers to resting-state *rCBF*, calculated as the average *rCBF* value over 2 minutes before NP. Bar heights are the mean values and error bars the s.d. over five animals. Horizontal dashed lines indicate maximum and minimum *rCBF* levels (given by the maximum bar height and minimum bar height across all time points and both anesthetics). (**E**) Bar plots of $\Delta rCBF$ values under isoflurane (dark gray) and propofol (white bars) at the same characteristic time points (a to h). The relative changes, $\Delta rCBF$, were calculated on a % scale with 0% taken as the resting-state baseline *rCBF* before needle prick, irrespective of the anesthesia regimen. More details about the relative $\Delta rCBF$ can be found in Supplementary Information S5. Significance of the factor 'anesthesia' on the levels of $\Delta rCBF$ and *rCBF* within each different time point was tested by multiple pairwise comparisons after two-way repeated measures analysis of variance: $^{*}P < 0.05$, $^{**}P < 0.01$, $^{***}P < 0.001$.

Electrophysiological Measurements in Rats

Electrode preparation and signal acquisition. Glass microelectrodes of 2.5–3 μm tip diameter were filled with 1 mol/L solution of sodium chloride (buffered at pH = 7). The microelectrodes were implanted through a small durectomy (~ 0.2 mm diameter) at a depth of 500 μm in half of the animals in each experimental group (Figure 1A). The presence of an implanted microelectrode did not influence the *rCBF* responses. Direct current (DC) and electrocorticogram (ECoG) were measured versus a subcutaneous sintered Ag/AgCl wire electrode that served as reference.

Data analysis. The mean value of the DC potentials over 2 minutes pre-CSD induction was taken as 0 mV and the amplitude of the DC shifts

Table 1. Systemic variables in various conditions of anesthesia and upstream blood supply

Experimental group	*Brain blood supply*	*Anesthesia*	n	*MABP (mm Hg)*	*PaO_2 (mm Hg)*	*$PaCO_2$ (mm Hg)*	*pH*
1	Normal	Isoflurane	5	95.2 ± 12.8	161.9 ± 12.5	43.2 ± 6.5	7.40 ± 0.06
		Propofol	5	106.3 ± 19.0*	152.4 ± 18.3	54.1 ± 6.1	7.33 ± 0.03
2	Normal	Isoflurane	5	83.7 ± 4.8	115.1 ± 34.7	40.5 ± 3.9	7.42 ± 0.03
		Propofol	4	96.3 ± 10.4	141.7 ± 42.2	49.0 ± 3.2**	7.33 ± 0.03***
3	Normal	Isoflurane	5	82.0 ± 15.7	153.0 ± 22.5	46.3 ± 6.6	7.41 ± 0.05
	CCA1		5	86.1 ± 13.5	142.2 ± 20.9	47.9 ± 6.4	7.40 ± 0.05
	CCA2		4	85.1 ± 22.8	146.0 ± 20.0	42.0 ± 3.6	7.40 ± 0.07
4	MCAo	Isoflurane	2	97.0 ± 21.5	142.6 ± 71.5	42.3 ± 3.6	7.41 ± 0.06
		Propofol	7	128.8 ± 17.4	133.8 ± 20.2	49.0 ± 8.5	7.35 ± 0.05

CCA, common carotid artery; MABP, mean arterial blood pressure; MCAo, middle cerebral artery occlusion. Isoflurane was maintained at 1.5% to 2% and propofol was infused via tail vein at 38 mg/kg per hour. All values are given as mean ± s.d. Arterial blood gas data are the average of the samples taken in each animal before each needle prick (groups 1 and 3) or before KCl application (group 2) or hourly (group 4). MMABP is the average over the full recordings in each condition. In all conditions, the systemic variables were within normal range. A paired *t*-test was performed between isoflurane and propofol in group 1, an unpaired *t*-test for groups 2 and 4, and a one-way repeated measures analysis of variance was performed in group 3 for factor 'blood supply' (normal, unilateral CCA ligation or bilateral CCA ligation). $^{*}P<0.05$, $^{**}P<0.01$, $^{***}P<0.005$.

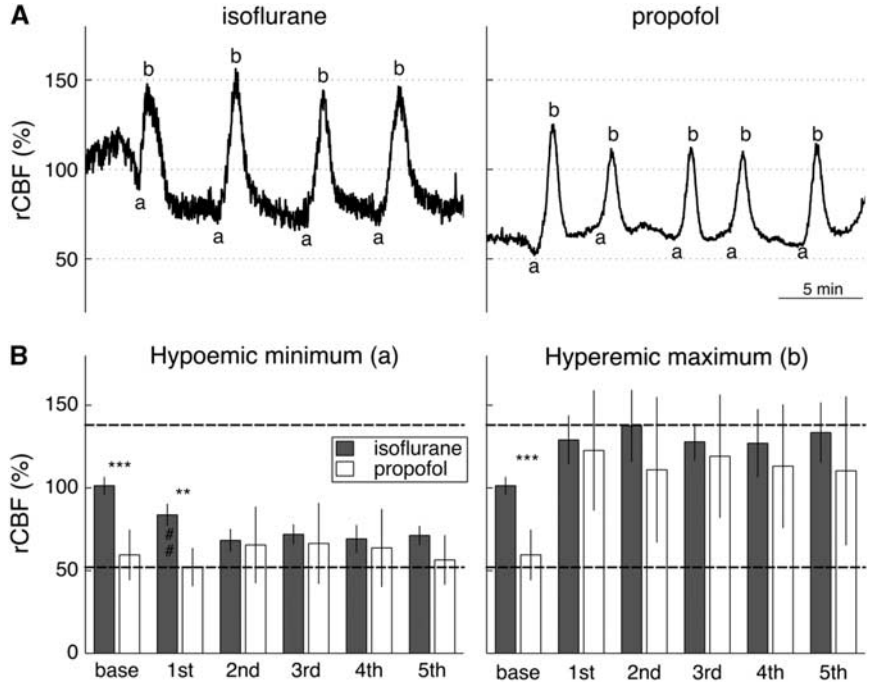

Figure 2. Regional cerebral blood flow (*rCBF*) response to multiple cortical spreading depolarizations (CSDs) under isoflurane or propofol anesthesia. (**A**) Typical *rCBF* responses to CSDs induced by epidural application of 3 mol/L KCl under isoflurane (left) and under propofol (right) (experimental group 2). We here show the *rCBF* responses from the ROI shown in Figure 1A. Note the lower frequency of CSD occurrence under isoflurane in comparison with propofol.[44] As CSDs recurred within 5 minutes, only points a and b, as defined in Figure 1, were analyzed. The same *rCBF* scale as in Figure 1 was used, 100% being baseline *rCBF* under isoflurane before KCl application. (**B**) Bar plot of the average ± s.d. *rCBF* values for points a (left) and b (right) across all isoflurane ($n=5$) and all propofol ($n=4$) animals, respectively. Point 'base' refers to the resting-state *rCBF*, calculated as the average ICT value over 2 minutes before KCl application (given 100% for isoflurane). Unpaired *t*-test between base *rCBF* in animals anesthetized with isoflurane and those with propofol was significant ($^{***}P<0.001$). Horizontal dashed lines indicate maximum and minimum *rCBF* measured across all animals. Significance for ANOVA *post hoc* pairwise multiple comparison for the factor 'anesthesia' is indicated as $^{**}P<0.01$, and for factor 'SD number' as $^{\#\#}P<0.01$.

calculated relative to this value. The duration of the DC shift was given by the width at half maximum. The power of the ECoG signal was calculated by taking the square of the ECoG signals between CSD.

Statistical Analysis

All data are presented either as individual data points or mean values ± s.d.

The physiologic variables, electrophysiological characteristics of the CSDs and their velocity of propagation were compared between isoflurane and propofol using a paired *t*-test for group 1 and unpaired *t*-test for group 2.

The *rCBF* and Δ*rCBF* data were analyzed using a two-way repeated measures analysis of variance for factors 'anesthesia' in groups 1 and 2 ('blood supply' in group 3) and factor 'time' in group 1 and 3 ('CSD number' in group 2). Tests for normality (Shapiro–Wilk test) and equal variance (Levene's median test) passed. Analysis of variance was followed by an all pairwise multiple comparison procedure (Holm–Sidak method).

Linear regressions were performed with the positive slope of *rCBF* response as dependent variable and pre-CSD *rCBF* levels as independent variable in experimental groups 3 and 4. The Pearson product–moment correlation coefficient was calculated to indicate the degree of linear dependence between the variables. Correlations between the positive slope of *rCBF* response and electrophysiological variables were assessed by Spearman rank order correlation (group 4 and clinical data).

For all statistical inferences, a P-value < 0.05 was considered statistically significant.

RESULTS

Systemic Variables

All experimental groups were within normal range for blood gases and mean arterial blood pressure. Propofol tended to increase $paCO_2$ and decrease pH, while slightly increasing blood pressure (Table 1).

Regional Cerebral Blood Flow Response to Cortical Spreading Depolarization under different Microvascular Tone Conditions

To modify the local microvascular tone, we used two different anesthetics, isoflurane and propofol, and induced CSDs, either by sequential needle pricks or KCl cotton ball (experimental groups 1 and 2, respectively). In both groups, resting-state rCBF values (point 'base', calculated as the average *rCBF* value over 2 minutes before needle prick) were much lower under propofol than under isoflurane, which was reflected by a significant impact of factor 'anesthesia' on *rCBF* ($F(1,32) = 13.5$; $P = 0.021$; significant difference between isoflurane and propofol at time point base).

Successful induction of CSD waves was verified by intracortical DC shifts and transient suppression of the power of the ECoG signals (Figure 1B). Amplitudes and durations of the DC shifts, as well as propagation velocities were similar under propofol and isoflurane and alike previously reported values.[5,20] With the depolarizations, we observed concomitant waves of *rCBF* alterations (Figure 1B).

Although starting from different resting-state levels, the *rCBF* levels during passage of a single CSD wave were remarkably similar between both anesthetics (experimental group 1, Figures 1C and 1D). To quantify the *rCBF* responses, eight characteristic time points (a to h) were defined (see insert in Figure 1C) and three distinct phases could be distinguished: an initial hypoemia (point a), a transient hyperemia (point b) followed by a prolonged hypoperfusion (commonly designated as 'oligemia') (points c to h at 5, 10, 20, 30, and 60 minutes post CSD induction). In particular, both responses reached the same maximum *rCBF* value of $127.5 \pm 38.2\%$ for isoflurane versus $119.8 \pm 27.2\%$ for propofol (no significant difference between propofol and isoflurane at time point b). Likewise, both responses were similar during the first 30 minutes after the needle prick (points c to f) with *rCBF* at its lowest value, ranging from 54.9% to 62.9% under isoflurane versus 44.7% to 57.8% under propofol (no significant differences at time points c–f). Differences between anesthetics were only found at resting state, onset and long after the passage of the CSD wavefront (significant differences at time points a, g, and h). In other words, the passage of the CSD wave abolished the anesthesia differences. Possible confounding effects of inducing CSDs by sequential needle pricks in one and the same animal were ruled out (Supplementary Figure S1).

The *rCBF* responses to multiple CSDs were also very similar between the two anesthesia regimens (experimental group 2, Figure 2). Before CSD induction, resting-state *rCBF* was significantly lower under propofol compared with isoflurane (unpaired t-test: $t(7) = -7.3$, $P < 0.001$). Once CSDs propagated, all differences were abolished. Two-way repeated measures analysis of variance with factors 'anesthesia' and 'CSD number' indeed revealed no significant effect of factor 'anesthesia' on *rCBF* at CSD minimum (time point a: $F(1,28) = 1.9$; $P = 0.213$) and CSD maximum (time point b: $F(1,28) = 0.7$; $P = 0.433$). Except at onset of the first CSD, there was also no difference between successive CSDs, with no overall significant effect of factor 'CSD number' (time point a: $F(4,28) = 1.1$; $P = 0.372$ and time point b: $F(4,28) = 0.6$; $P = 0.660$). During the passage of CSD waves, *rCBF* varied within well-defined minimum and maximum *rCBF* boundary values of 52% and 138%, respectively (horizontal dashed lines on Figure 2B). Comparable minimum and maximum *rCBF* limits could be inferred from the single CSD responses (horizontal dashed lines on Figure 1D).

Regional Cerebral Blood Flow Response to Cortical Spreading Depolarization Relative to Baseline

As it is common to present *rCBF* responses relative to baseline pre-CSD values, we also analyzed the relative *rCBF* changes during the passage of a CSD wave, i.e, $\Delta rCBF$ (Figure 1E). Here, relative changes in *rCBF* in response to individual CSD, i.e., $\Delta rCBF$ (Figure 1B and 1E) were given by the changes of ICT relative to each pre-CSD ICT taken as $\Delta rCBF = 0\%$, irrespective of the anesthesia regimens (Figure 1E, point 'base'). In these terms, striking differences in the magnitudes of the responses could be observed between the two anesthesia regimens (factor 'anesthesia': $F(1,32) = 151.4$; $P < 0.001$). These differences in relative changes were not because of the order of the sequence of CSD inductions (Supplementary Figure S2). The divergence in $\Delta rCBF$ was particularly striking at the hyperemic maximum (point b), where $\Delta rCBF_b = +32.1 \pm 35.5\%$ under isoflurane compared with $+146.1 \pm 27.5\%$ under propofol (significant difference between isoflurane and propofol at time point b, and also c–g). After the hyperemia, the oligemic phase was more prominent under isoflurane (down to $-45.1 \pm 11.7\%$ from baseline) than under propofol (down to $-19.3 \pm 20.4\%$ at the most).

Regional Cerebral Blood Flow Response to Cortical Spreading Depolarization under different Upstream Blood Supply Conditions

To test the effect of upstream blood supply on the *rCBF* response to CSD, we altered the global blood supply to the brain by successive ligation of the left and right CCAs, while maintaining the animals under isoflurane anesthesia (experimental group 3). Both types of CCA ligation significantly changed the *rCBF* responses to CSD (factor 'blood supply': $F(2,18) = 13.4$, $P = 0.006$).

Ligation of the left CCA resulted in a drop in *rCBF* in the left hemisphere as observed in previous studies.[21] This reduction in perfusion was substantial, falling to $66.5 \pm 11.4\%$ *rCBF* in the territory of the MCA (Figures 3B and 4D). A needle prick elicited a CSD wave with similar DC shift and duration as under normal blood supply. The *rCBF* response was also triphasic but shifted to lower *rCBF* levels (trace CCA1 in Figure 3B). The initial brief hypoperfusion reached lower *rCBF* than under normal blood supply to the brain ($43.2 \pm 24.1\%$ versus $79.9 \pm 19.0\%$) but the relative drop was of similar magnitude. The transient hyperemia was, however, significantly smaller in magnitude (comparison between normal blood supply and CCA1 was significant within point b, point of maximum hyperemia). Remarkably, *rCBF* values during the long-term hypoperfusion phase were very similar before or after unilateral CCA ligation (comparison between normal blood supply and CCA1 was not significant at 30 minutes) (Figures 3E).

When the right CCA was additionally ligated, global hypoperfusion of the whole brain became apparent. Regional cerebral blood flow fell to $49.5 \pm 10.2\%$ in the territory of the MCA (Figures 3B and 4D), a value comparable with previous studies.[22] Despite an almost identical *rCBF* resting-state level compared with propofol ($49.3 \pm 9.5\%$), the *rCBF* response to the CSD wave was different, the transient hypoemia being intensified and the following *rCBF* rise reaching baseline value (trace CCA2 in

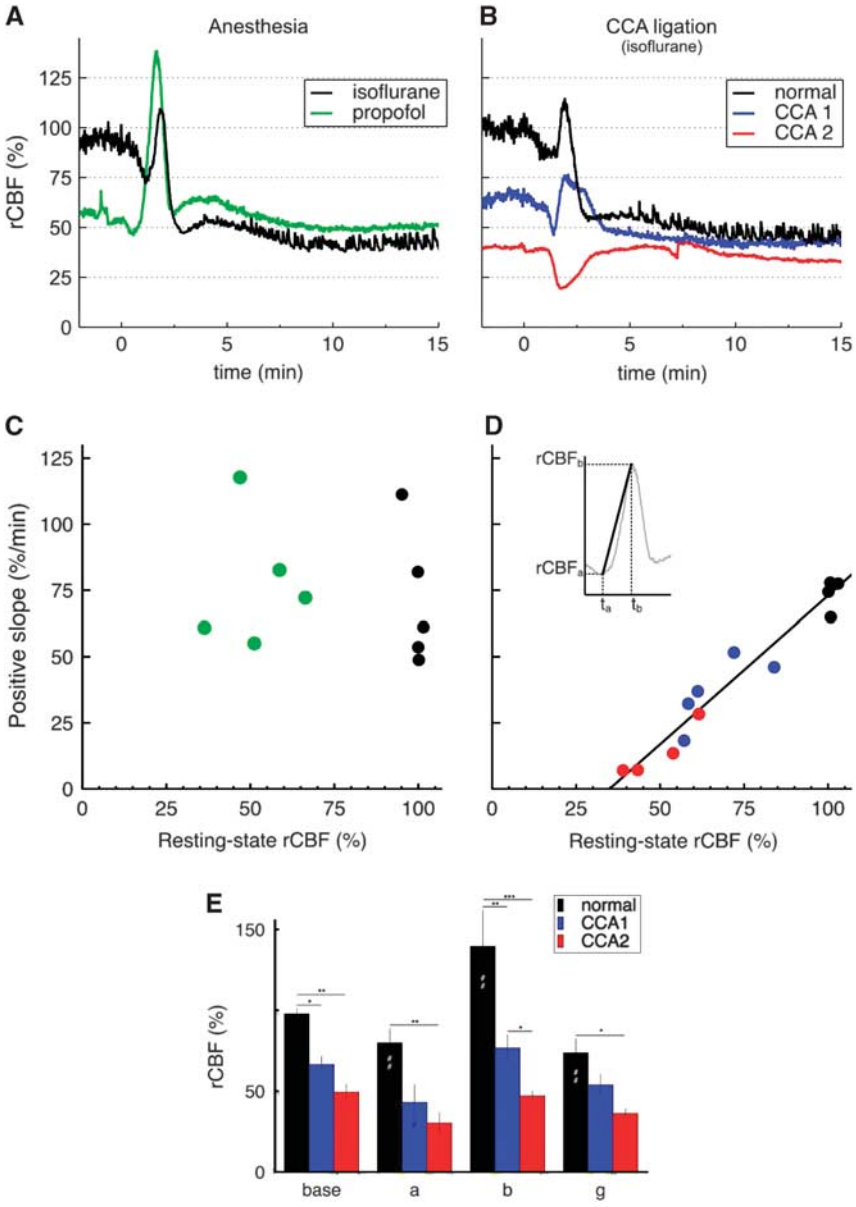

Figure 3. Regional cerebral blood flow (*rCBF*) response after common carotid artery (CCA) ligation and correlation between the positive slope of *rCBF* response and resting-state *rCBF*. (**A**) Exemplar *rCBF* responses to cortical spreading depolarization (CSD) induced by sequential needle pricks under different anesthesia regimens (experimental group 1): either isoflurane (black) or propofol (green). (**B**) Exemplar *rCBF* responses to CSD induced by sequential needle pricks under different upstream blood supply conditions (experimental group 3): normal blood supply to the brain (black), after ligation of the left CCA (blue), and after ligation of both CCA (red). All *rCBF* time courses shown were extracted from the same region of interest defined in Figure 1A, i.e., lying in the territory of the middle cerebral artery. Regional cerebral blood flow 100% was taken as the average inverse correlation time value 2 minutes before needle prick under isoflurane and normal blood supply to the brain. Time 0 is the time of each respective needle prick. See also Supplementary Movie. (**C**) Scatter plots of the positive slope of *rCBF* response versus resting-state *rCBF* in cases of different anesthesia regimens in $n = 5$ animals (experimental group 1, black for isoflurane, green for propofol). (**D**) Scatter plots of the positive slope versus resting-state *rCBF* in cases of different brain blood supply for $n = 5$ animals (experimental group 3). Same color code as in (**B**). In one animal, a spontaneous CSD wave propagated after bilateral CCA ligation, and thus no third needle prick was performed (only four red points). Resting-state *rCBF* values were defined as the average *rCBF* values 2 minutes prior each needle prick (with 100% *rCBF* taken under isoflurane with normal blood supply). The positive slope was calculated for each *rCBF* wave by the ratio $(rCBF_b - rCBF_a)/(t_b - t_a)$ (see insert). Parameters for the linear regression in (**D**) are as follows: $y = 1.12 \times x - 39.3$, $R^2 = 0.947$. (**E**) Cerebral blood flow response to CSD under normal conditions ($n = 5$) and during unilateral (CCA1, $n = 5$) and bilateral (CCA2, $n = 4$) CCA ligation. Labeling of time points as in Figure 1 (a = min, b = max, g = 30 minutes). Significance of the factor 'ligation' on the levels of *rCBF* within each different time point was tested by multiple pairwise comparisons after two-way repeated measures analysis of variance: $^{*}P < 0.05$, $^{**}P < 0.01$, $^{***}P < 0.001$. ($^{\#}P < 0.05$) and ($^{\#\#}P < 0.01$) indicate significant differences to time point 'base' in each ligation group.

Figure 3B). Moreover, in the bilateral CCA ligation case, we measured a prolonged DC shift of 7–8 minutes (compared with 22.5 ± 3.0 seconds under normal blood supply). The *rCBF* responses to CSD waves induced by needle pricks under these three different upstream blood supply conditions are shown in the Supplementary Movie.

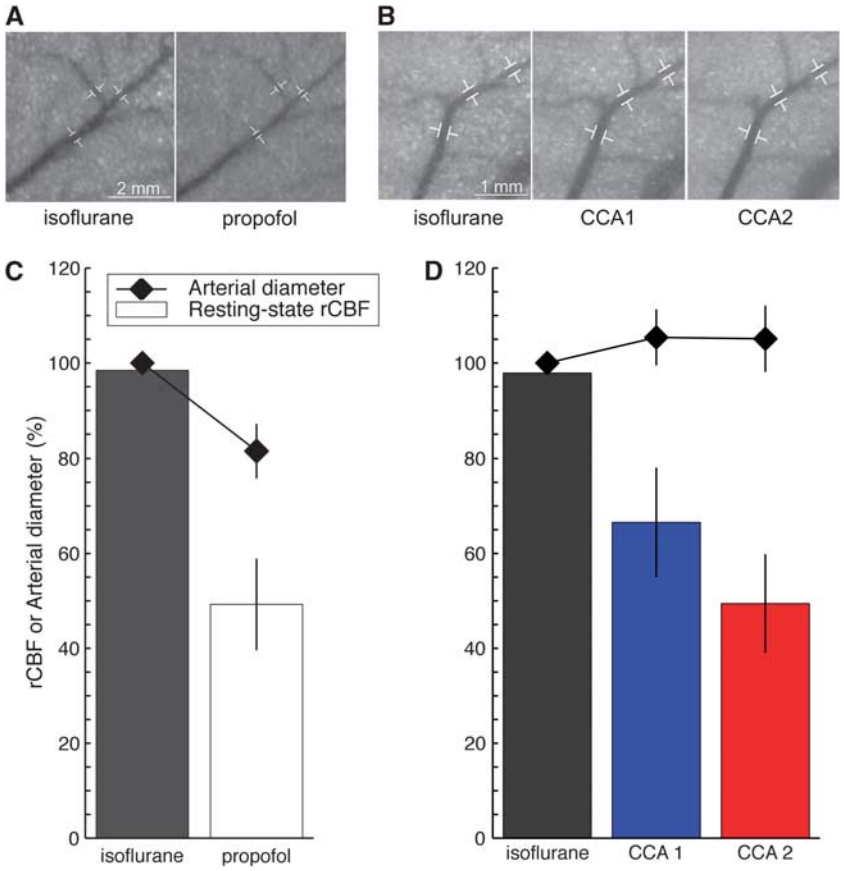

Figure 4. Regional cerebral blood flow (*rCBF*) and microvascular tone. Close-up on the middle cerebral artery (MCA) before induction of the cortical spreading depolarization (CSD) under different anesthesia regimens, isoflurane and propofol (**A**), or under different upstream blood supply conditions (**B**). These images show speckle contrast temporally averaged over 40 seconds. Sequential common carotid artery (CCA) ligations were performed under isoflurane. Common carotid artery 1 (CCA1) refers to the ligation of the left CCA. Common carotid artery 2 (CCA2) refers to the ligation of both CCAs. Three segments along the distal portion of the MCA were used to quantify arterial diameter changes, as shown by the white markers. Resting-state *rCBF* (bars, $n = 5$ animals) and arterial diameter (diamonds) when the anesthesia regimen was modified (**C**) or when the upstream blood supply to the brain was altered (**D**). Resting-state *rCBF* was the averaged *rCBF* value before needle prick calculated across $n = 5$ animals from group 1 (**C**) or across $n = 5$ animals from group 3 (**D**). Regional cerebral blood flow 100% refers to isoflurane *rCBF* under normal upstream blood supply. Similarly, the arterial diameter measured under isoflurane at normal blood supply before needle prick was set to 100%. Changes from this 100% arterial diameter are reported as mean ± s.d. for the three segments of the MCA (shown in **A** and **B**). Note that the region of interest for *rCBF* calculation was intentionally not placed on a major blood vessel to reflect tissue *rCBF*. Microvascular tone and resting-state *rCBF* were closely related under normal blood supply to the brain but dissociated when the CCAs were ligated and upstream blood supply reduced.

Regional Cerebral Blood Flow and Microvascular Tone

Anesthetic regimens and CCA ligations, respectively, established two different conditions that led to two almost identical *rCBF* levels. In the first case, propofol reduced *rCBF* levels to 49.3 ± 9.5% by constriction of the arteries and arterioles (groups 1 and 2). We estimated that the diameters of distal branches of the MCA were reduced to 81.5 ± 5.7% of that under isoflurane (Figure 4A–C). In the second case (group 3), bilateral CCA ligation decreased *rCBF* levels to 49.5 ± 10.2% despite full dilation of the blood vessels. We measured slightly increased diameters to 105.1 ± 7% of normal isoflurane (Figures 4B and 4D). In that case, the reduction in *rCBF* was solely because of the hindered delivery of blood to the tissue (only supplied by the basilar artery). Importantly, the origin of the blood flow change (microvascular tone or upstream blood supply) determined the shape of the *rCBF* response to a CSD wave (Figures 3A and 3B).

Positive Slope of Regional Cerebral Blood Flow Response to Cortical Spreading Depolarizations Indicates Upstream Blood Supply

At equivalent *rCBF* levels, a restriction of the upstream blood supply severely limited the extent and steepness of the positive slope of *rCBF* response after a CSD wave (Figure 3B). We characterized this effect by measuring the 'positive slope', i.e., the *rCBF* increase per unit of time in response to a CSD (see insert in Figure 3D). In the CCA ligation group (experimental group 3), we found a significant linear dependency between the positive slope in response to CSD and resting-state *rCBF* values (Figure 3D; linear regression: positive slope = 1.12 *rCBF* − 39.3; $R^2 = 0.947$). In that case, resting-state *rCBF* levels reflected solely upstream blood supply because blood vessels were fully dilated. In the anesthesia group (group 1), resting-state *rCBF* levels were influenced by microvascular tone. In that case, there was no correlation between resting-state *rCBF* values and positive slope (Figure 3C). In fact, the positive slopes were almost identical under isoflurane and propofol, 71.3 ± 25.6%/minute and 77.7 ± 24.7%/minute respectively, with no significant difference (paired *t*-test: $t(4) = -0.356$, $P = 0.740$). Under the different anesthesia regimens, the upstream blood supply was the same and therefore, the capacity to increase *rCBF* in response to energy demand was the same, as revealed by identical positive slopes of *rCBF* response to CSD.

Positive Slope of Regional Cerebral Blood Flow Response as a Marker of Tissue Condition in Experimental Embolic Stroke

In the experimental focal ischemia group (group 4), we modified upstream blood supply by embolic occlusion of the middle cerebral artery (MCA). Immediately after occlusion, a spatial pattern of gradual reduction in *rCBF* could be observed with the establishment of an ischemic focus in the arterial territory of the MCA. Over the courses of the experiments, spontaneous *rCBF* waves propagated across the cortical surface. These *rCBF* waves corresponded to CSDs, as verified by microelectrode extracellular recordings. In total, the number of spontaneous CSD waves varied among all nine animals from 1 to 17, during up to 3-hour observation. The spatiotemporal patterns of these CSD waves that arise spontaneously after MCAo have been well characterized in previous studies.[7,15] Here, we observed similar waveforms and, in all cases, the *rCBF* wave patterns were comparable with those observed in the CCA ligation group (compare Figure 5 with Figure 3B).

In two animals under isoflurane, we found a significant linear dependency between CSD-associated positive slopes of *rCBF* response and *rCBF* levels before each CSD wave (Figure 5D; linear regression: positive slope = 1.24 *rCBF* − 62.1; $R^2 = 0.87$). The slope and intercept of the regression line were somewhat different from the ones found in the CCA ligation group, presumably because the collateral flow patterns differed in the two conditions.

In all other animals, because of frequent *rCBF* waves after MCAo (3 to 12-minute intervals), no obvious evolution of perfusion gradients was observed (Figure 5E). However, clear zonal gradients could be established based on the positive slopes measured in the different ROIs (Figure 5F bottom). In contrast to relatively stable *rCBF* levels, the positive slopes decreased markedly with time (Figure 5F). Concomitantly, the duration of the DC shifts increased (from 1.5 minutes for the first CSD to 4 minutes for the last) and the amplitude of the power of the ECoG signals dropped (from 17.4 mV^2 at 5 minutes post MCAo to 2.1 mV^2 by 2.5 hours post MCAo). We also found good correlations between these electrophysiological parameters and the positive slopes of the ROI closest to the microelectrode (Figure 5G, Spearman rank order correlation for hyperemic slope and DC shift duration: $R = -0.78$, $P = 0.00897$; for hyperemic slope and EEG power amplitude: $R = 0.72$, $P = 0.0248$). An additional MCAo case is given in Supplementary Figure S3.

DISCUSSION

Distinguishing Upstream Blood Supply and Local Microvascular Tone

Regional cerebral blood flow is one accessible measure for estimating brain tissue conditions, whether by imaging or local probe measurements.[23] However, *rCBF* is determined both by upstream blood supply and by local microvascular tone. The latter applies to all microvessels at the site of metabolite exchange, while the former is controlled by all upstream vascular branches that feed blood to the local territory. The same *rCBF* levels may correspond to very different conditions of upstream blood supply. There are two extreme situations:

i If the upstream blood supply is high, normal levels of *rCBF* are associated with constricted local microvessels.
ii If the upstream blood supply is low, normal levels of *rCBF* are maintained by highly dilated local microvessels.

Although the *rCBF* value is the same in both situations, the dynamic range of *rCBF* is quite different. In case (i), *rCBF* can be easily increased by dilation of local microvessels to respond to an increased energy demand. In case (ii), local microvessels are already at maximum dilation and *rCBF* cannot be raised to respond to an increased energy demand. The limited capacity to raise *rCBF* in case (ii), which impairs brain function locally, is not discernible in the resting-state *rCBF* levels. The reduction of the capacity to raise *rCBF* when reducing upstream blood supply has also been reported by Baker *et al*[24] who observed an attenuation of the *rCBF* response to electrical forepaw stimulation as they gradually occluded the CCAs.

Cortical spreading depolarizations reveal upstream blood supply. The most typical feature of the *rCBF* response to a CSD, given a normal blood supply to the brain, is its propagating hyperperfusion as a result of local vasodilation.[4,5] The hyperemic response to a CSD has always been reported to be very large, and substantially bigger than under other physiologic stimulation paradigms. The widely accepted reason for this is that a CSD event is a complete local depolarization with massive changes in ion homeostasis lasting over tens of seconds. The re-establishment of the ion concentration gradients needs a considerable amount of energy, which would entail a significant increase in *rCBF* to provide the energy substrates. We suggest that the vessel dilation during

Figure 5. Positive slope of regional cerebral blood flow (*rCBF*) response in experimental stroke model. (**A**) Typical laser speckle image of the left hemisphere through thinned skull prepared for middle cerebral artery occlusion (MCAo). Six regions of interest (ROIs) (colored circles) were placed along distal branches of the middle cerebral artery (MCA) (avoiding major blood vessels) at various distances relative to the ischemic focus (close to focus in red, far in green). A microelectrode (direct current (DC)) was also implanted in some animals, at various positions along the distal portion of the MCA. When *rCBF* waves hit the microelectrode, we observed a DC shift and a transient depolarization in the electrocorticogram (ECoG) activity, indicating that the *rCBF* waves were cortical spreading depolarization (CSD) events. (**B**) Postmortem examination of the location of the macrosphere (indicated by the black arrow). The macrosphere was typically trapped at the bifurcation of MCA and anterior cerebral artery. (**C**) Exemplar *rCBF* traces in three ROIs in animal 1 (same color code as in (**A**)). In this case, clear zonal *rCBF* gradients were observed immediately after occlusion. These *rCBF* gradients remained stable during the whole course of the experiment. Time 0 was defined as the time of occlusion (MCAo). Before occlusion, the common carotid artery (CCA) was ligated, so *rCBF* levels were of 66.5%. (**D**) Correlation between the positive slope of the *rCBF* response to CSD and the pre-CSD *rCBF* levels in animals 1 (closed symbol) and 2 (open symbol), where MCAo was induced under isoflurane. For each ROI (same color code as in (**A**)), *rCBF* (in between successive CSD waves) was stable over time (see **C**), and we defined the pre-CSD *rCBF* level as the average value of *rCBF* during 2 minutes before each CSD. We also calculated a positive slope for each CSD wave (see insert Figure 3D) in two animals. Parameters of the linear regression were as follows: $y = 1.24 \times x - 62.1$, $R^2 = 0.87$. (**E**) Exemplar *rCBF* traces in animal 3 (under propofol). After an hour gap following the first concentric CSD, circumferential CSD waves frequently propagated, so that the *rCBF* levels were highly influenced by the CSD waves. (**F**) Inter-CSD *rCBF* levels and positive slope over time (animal 3). Regional cerebral blood flow levels of different ROIs were similar (top) while the positive slope showed clear differences (bottom). The positive slope decreased with time, while *rCBF* remained quite stable. (**G**) Correlation of the positive slope with the electrophysiological variables measured with the microelectrode shown in (**A**) in animal 3. Direct current durations were calculated for each CSD wave as the width at half maximum. The ECoG power was calculated between successive CSDs. Note that the *x*-axis for the ECoG power is reversed, going from high power to low power values. The DC duration and the positive slope were negatively correlated, with decreasing positive slopes for increasing DC durations (Spearman rank order correlation: $R = -0.78$, $P = 0.00897$). The power of the ECoG signal and the positive slope were positively correlated (Spearman rank order correlation: $R = 0.72$, $P = 0.0248$).

CSD-induced hyperemia is maximal and thereby causes (at normotension) not only huge but maximal achievable values of *rCBF*. We indeed measured, in 24 animals and 80 induced CSDs, an increase in *rCBF* that reached in all cases the same maximum value of 140% to 150% of resting-state isoflurane *rCBF* (Figures 1 and 2). According to absolute resting-state *rCBF* under 1.5% to 2% isoflurane (150 to 180 mL/minute per 100 g),[25] we would estimate the maximum *rCBF* after a CSD to be 220 to 270 mL/minute per 100 g. Remarkably, studies from other groups all found the same *rCBF* peak value, using a variety of animal preparations, various anesthetic agents, and other *rCBF* measurement methods. For instance:

- halothane anesthesia: *rCBF* increased to 2.1 times that of baseline,[26] i.e., 210 mL/minute per 100 g for 100 mL/minute per 100 g resting-state *rCBF*[27]
- alpha-chloralose anesthesia: *rCBF* increase of 240% above baseline,[5] i.e., 220 mL/minute per 100 g given their resting-state *rCBF*[28]

Other examples can be found in the review by Busija *et al*.[29] It is very unlikely that the same *rCBF* level would be reached in all

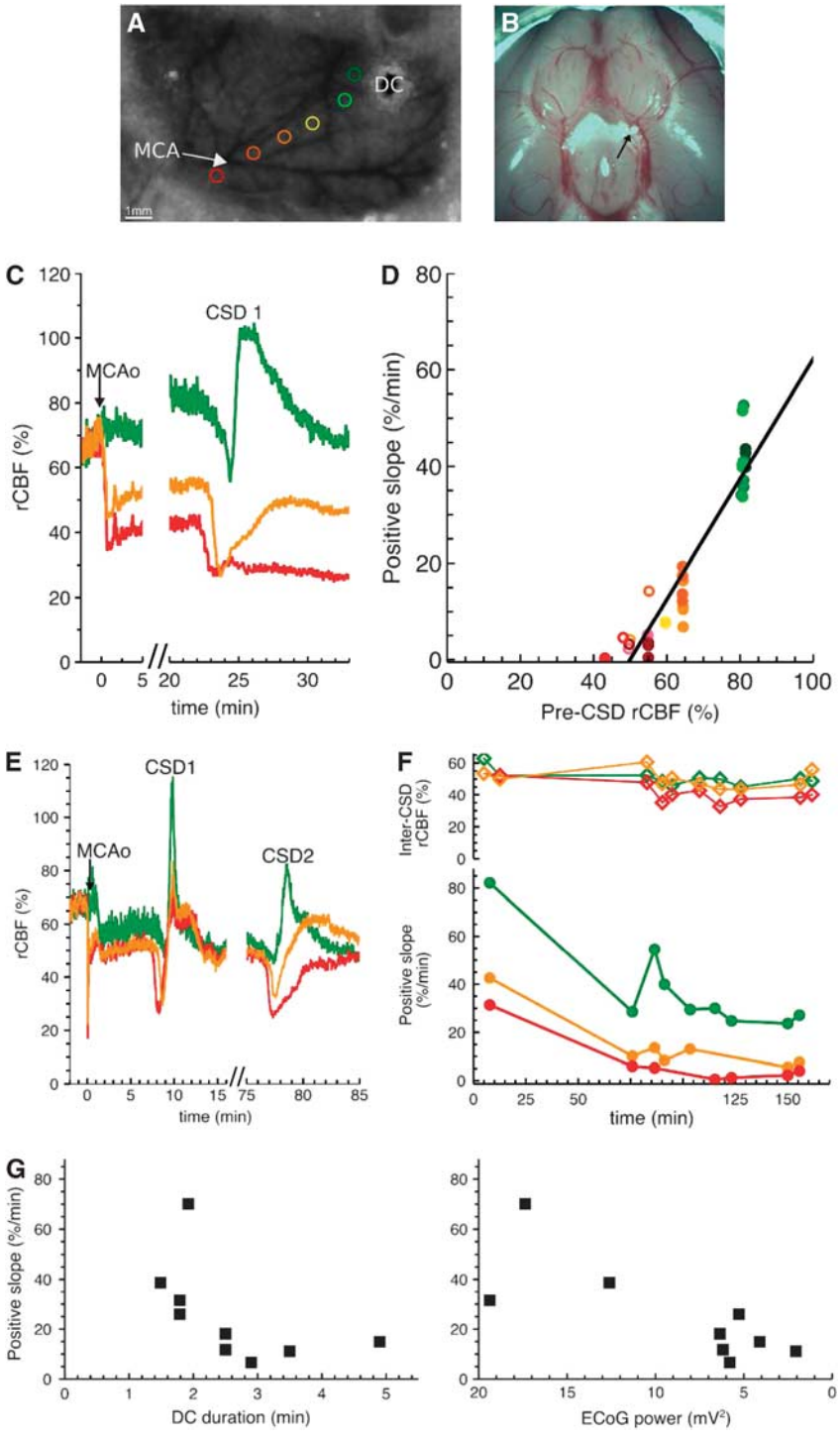

experimental conditions if that level did not correspond to a physiologically well-defined upper limit.

This *rCBF* increase is caused by dilation of pial arteries and arterioles.[30–32] Although blood vessels are already fully dilated within 1–2 seconds after the depolarization,[33] it takes ~1 minute to reach the maximum *rCBF* value after onset of the hyperemia (Figure 1). This would suggest that the rate-limiting step of the hyperperfusion response would be the supply of blood to the fully dilated microvessels, which we refer to as the upstream blood supply. Hence, the increase of *rCBF* per time, i.e., the positive slope of *rCBF* response, is a function of the upstream blood supply.

Sukhotinsky *et al.*[34] reported a dependence of *rCBF* response during CSD on blood pressure, which directly controls cerebral perfusion pressure and therefore upstream blood supply. Similarly, Baker *et al.* analyzed changes of CBF in response to somatosensory stimulation during different levels of global ischemia.[24] The magnitude of CBF response decreased and time-to-peak increased as a function of the ischemic level. The authors concluded: 'upstream vascular clamping or hypotension causes the local vasculature to dilate with potential negative implications for further dilation in response to neuronal activation.'[24] In other words, despite likely similar vasosignaling, CBF responses were different because of restriction on the upstream blood supply.

It should be noted, however, that there is recent evidence that ischemic conditions could trigger contraction of some pericytes that would partially limit capillary flow to the metabolite exchange point.[35,36] In this case, the capacity to raise CBF in response to increased energy demand would be limited at the capillary level upstream of the metabolite exchange point. Yemisci *et al.*[36] observed normal *rCBF* levels measured by LDF even when capillary flow was reduced. Thus measuring *rCBF* did not reveal the limit in blood supply.

Application to Pathologic Conditions

In pathologic conditions, such as focal ischemia, the transient CBF response to CSD is modified with decreasing distance to the ischemic core: in the distant periphery, *rCBF* increases almost monophasically (spreading hyperemia), whereas near the core, it is an almost monophasic decrease of *rCBF* (spreading ischemia), and in the zones in between, biphasic responses have been measured.[9] Similar patterns were observed in brain injury patients, where spontaneously propagating CSDs with prolonged DC shifts and spreading ischemia could contribute to lesion progression.[37,38] The transition from physiologic hemodynamic response (spreading hyperemia) to inverse hemodynamic response (spreading ischemia) is usually explained by alterations of CSD-related vasoactive signaling in pathologic conditions. In particular, there is experimental evidence that the combination of elevated baseline $K+$ concentrations and impaired NO signaling can cause spreading ischemia in response to induced CSD.[39] Such conditions are fulfilled after subarachnoid hemorrhage where hemoglobin in the subarachnoid clot acts as an NO scavenger and potassium is released in the subarachnoid space.[38] Whether similar conditions are met after focal ischemia requires further study: possible vasoconstrictive mechanisms have been suggested[8] while significant rises in NO have also been measured acutely.[40]

We here suggest an alternative mechanism that could explain the various CBF responses to CSDs observed in physiologic and pathologic conditions: restriction of blood supply. Our hypothesis is that any CSD leads to two successive vasoactive signaling phases: (1) a very short vasoconstriction (point a, Figures 1–3), presumably caused by elevated extracellular level of potassium, followed by (2) a transient maximum vasodilation to deliver substrates to the depolarized cells for re-establishment of ion concentration gradients (point b, Figures 1–3). Under propofol, the vasoconstrictive phase is very limited, as the vessels are already constricted and vasoconstrictive signaling cannot constrict blood vessels much further (see further discussion in Supplementary S5). Conversely, if local vessels are dilated, for example to preserve local energy delivery when blood supply is reduced because of global or focal ischemia, the same CSD-related vasoactive signaling (short vasoconstriction followed by full vasodilation) would cause a marked initial hypoperfusion. In addition, because of limited blood supply, the rise of *rCBF* during the vasodilation phase takes much longer. Our CCA ligation experiments indeed show this type of hemodynamic response to CSD (Figure 3) and the positive slope linearly correlates with the capacity to raise blood flow, which is here directly determined by upstream blood supply.

In the case of focal ischemia, it was demonstrated in cats that the gradual transition from spreading hyperemia to spreading ischemia follows the decreasing gradient in blood flow with decreasing distance to the ischemic core.[9] We observed the same patterns in the animals under isoflurane after MCAo, where we suggest that, since vessels were fully dilated, the gradient in blood flow levels was directly linked to a progressive restriction in blood supply with increasing proximity to the occluded artery (Figure 5C). In that case, there was a direct linear relationship between pre-CSD *rCBF* levels and positive slope (Figure 5D), similar to the CCA case (Figure 3D). In the MCAo animals under propofol, there was no relation between pre-CSD *rCBF* and positive slope (Figure 5F). We would suggest that, over time, local blood vessels dilate further to compensate for reductions in upstream blood supply and maintain *rCBF* (such as in the green ROI on Figure 5F top panel). In these cases, the positive slope was correlated to DC shift durations and ECoG power (Figure 5G), that can be regarded as electrophysiological markers of tissue functional status.[41,42]

Clinically, we could measure the dynamic *rCBF* responses to spontaneous CSDs using a hybrid subdural strip combining electrodes and optodes that was previously used in a study in SAH patients[37] (see Supplementary S4). Similarly to the MCAo group, we found a significant correlation between positive slope of *rCBF* response and tissue functional status, as the injury developed over time: the positive slope decreased with prolongation of the duration of the ECoG suppression in two brain injury patients who presented with very different pathologies (subarachnoid hemorrhage and trauma) (Supplementary Figure S4E). As restoration of ECoG activity after spreading depolarization is energy dependent, the duration of ECoG depression until recovery is usually considered as an indirect indicator of the tissue energy status.[43] We would conclude that the positive slope is a marker for the capacity to raise blood flow in response to increased energy demand (such as that caused by a CSD) and is therefore a valuable indicator of tissue conditions. Whether this altered capacity to raise blood flow after brain injury is mainly due to the dysregulated release of vasoeffectors in pathologic conditions, or mainly due to the restriction of blood supply to the metabolite exchange point needs further examination. It is likely to be a combination of both.

DISCLOSURE/CONFLICT OF INTEREST

The authors declare no conflict of interest.

ACKNOWLEDGMENTS

The authors thank Dr Andrew Dunn for providing us with the laser speckle software.

REFERENCES

1 Vanzetta I, Grinvald A. Coupling between neuronal activity and microcirculation: implications for functional brain imaging. *HFSP J* 2008; **2**: 79–98.
2 Hertle DN, Dreier JP, Woitzik J, Hartings JA, Bullock R, Okonkwo DO *et al.* Effect of analgesics and sedatives on the occurrence of spreading depolarizations accompanying acute brain injury. *Brain* 2012; **135**: 2390–2398.

3 Feuerstein D, Manning A, Hashemi P, Bhatia R, Fabricius M, Tolias C *et al.* Dynamic metabolic response to multiple spreading depolarizations in patients with acute brain injury: an online microdialysis study. *J Cereb Blood Flow Metab* 2010; **30**: 1343–1355.
4 Lauritzen M. Regional cerebral blood flow during cortical spreading depression in rat brain: increased reactive hyperperfusion in low-flow states. *Acta Neurol Scand* 1987; **75**: 1–8.
5 Piilgaard H, Lauritzen M. Persistent increase in oxygen consumption and impaired neurovascular coupling after spreading depression in rat neocortex. *J Cereb Blood Flow Metab* 2009; **29**: 1517–1527.
6 Ayata C, Shin HK, Salomone S, Ozdemir-Gursoy Y, Boas DA, Dunn AK *et al.* Pronounced hypoperfusion during spreading depression in mouse cortex. *J Cereb Blood Flow Metab* 2004; **24**: 1172–1182.
7 Kumagai T, Walberer M, Nakamura H, Endepols H, Sué M, Vollmar S *et al.* Distinct spatiotemporal patterns of spreading depolarizations during early infarct evolution: evidence from real-time imaging. *J Cereb Blood Flow Metab* 2010; **31**: 580–592.
8 Shin HK, Dunn AK, Jones PB, Boas DA, Moskowitz MA, Ayata C. Vasoconstrictive neurovascular coupling during focal ischemic depolarizations. *J Cereb Blood Flow Metab* 2006; **26**: 1018–1030.
9 Strong AJ, Anderson PJ, Watts HR, Virley DJ, Lloyd A, Irving EA *et al.* Peri-infarct depolarizations lead to loss of perfusion in ischaemic gyrencephalic cerebral cortex. *Brain* 2007; **130**: 995–1008.
10 Fabricius M, Fuhr S, Bhatia R, Boutelle M, Hashemi P, Strong AJ *et al.* Cortical spreading depression and peri-infarct depolarization in acutely injured human cerebral cortex. *Brain* 2006; **129**: 778–790.
11 Dohmen C, Sakowitz OW, Fabricius M, Bosche B, Reithmeier T, Ernestus R-I *et al.* Spreading depolarizations occur in human ischemic stroke with high incidence. *Ann Neurol* 2008; **63**: 720–728.
12 Lauritzen M, Dreier JP, Fabricius M, Hartings JA, Graf R, Strong AJ. Clinical relevance of cortical spreading depression in neurological disorders: migraine, malignant stroke, subarachnoid and intracranial hemorrhage, and traumatic brain injury. *J Cereb Blood Flow Metab* 2011; **31**: 17–35.
13 Hartings JA, Watanabe T, Bullock MR, Okonkwo DO, Fabricius M, Woitzik J *et al.* Spreading depolarizations have prolonged direct current shifts and are associated with poor outcome in brain trauma. *Brain* 2011; **134**: 1529–1540.
14 Dunn AK, Bolay H, Moskowitz MA, Boas DA. Dynamic imaging of cerebral blood flow using laser speckle. *J Cereb Blood Flow Metab* 2001; **21**: 195–201.
15 Nakamura H, Strong AJ, Dohmen C, Sakowitz OW, Vollmar S, Sué M *et al.* Spreading depolarizations cycle around and enlarge focal ischaemic brain lesions. *Brain* 2010; **133**: 1994–2006.
16 Ayata C, Dunn AK, Gursoy-Ozdemir Y, Huang Z, Boas DA, Moskowitz MA. Laser speckle flowmetry for the study of cerebrovascular physiology in normal and ischemic mouse cortex. *J Cereb Blood Flow Metab* 2004; **24**: 744–755.
17 Li P, Ni S, Zhang L, Zeng S, Luo Q. Imaging cerebral blood flow through the intact rat skull with temporal laser speckle imaging. *Opt Lett* 2006; **31**: 1824–1826.
18 Abramoff MD, Magalhaes PJ, Ram SJ. Image processing with ImageJ. *Biophotonics Int* 2004; **11**: 36–43.
19 Meijering E. Biomedical IG of the SFI of T in L. FeatureJ 2003http://www.imagescience.org/meijering/software/fea.
20 Leão AAP. Spreading depression of activity in the cerebral cortex. *J Neurophysiol* 1944; **7**: 359–390.
21 De Ley G, Nshimyumuremyi JB, Leusen I. Hemispheric blood flow in the rat after unilateral common carotid occlusion: evolution with time. *Stroke* 1985; **16**: 69–73.
22 Tsuchiya M, Sako K, Yura S, Yonemasu Y. Cerebral blood flow and histopathological changes following permanent bilateral carotid artery ligation in Wistar rats. *Exp brain Res* 1992; **89**: 87–92.
23 Panerai RB. Assessment of cerebral pressure autoregulation in humans - a review of measurement methods. *Physiol Meas* 1998; **19**: 305–338.
24 Baker WB, Sun Z, Hiraki T, Putt ME, Durduran T, Reivich M *et al.* Neurovascular coupling varies with level of global cerebral ischemia in a rat model. *J Cereb Blood Flow Metab* 2013; **33**: 97–105.
25 Maekawa T, Tommasino C, Shapiro HM, Keifer-Goodman J, Kohlenberger RW. Local cerebral blood flow and glucose utilization during isoflurane anesthesia in the rat. *Anesthesiology* 1986; **65**: 144–151.
26 Fabricius M, Akgoren N, Lauritzen M. Arginine-nitric oxide pathway and cerebrovascular regulation in cortical spreading depression. *Am J Physiol* 1995; **269**: H23–H29.
27 Lauritzen M. Long-lasting reduction of cortical blood flow of the brain after spreading depression with preserved autoregulation and impaired CO2 response. *J Cereb Blood Flow Metab* 1984; **4**: 546–554.
28 Masamoto K, Kanno I. Anesthesia and the quantitative evaluation of neurovascular coupling. *J Cereb Blood Flow Metab* 2012; **32**: 1233–1247.
29 Busija DW, Bari F, Domoki F, Horiguchi T, Shimizu K. Mechanisms involved in the cerebrovascular dilator effects of cortical spreading depression. *Prog Neurobiol* 2008; **86**: 379–395.
30 Leão AAP. Pial circulation and spreading depression of activity in the cerebral cortex. *J Neurophysiol* 1944; **7**: 391–396.
31 Brennan KC, Beltrán-Parrazal L, López-Valdés HE, Theriot J, Toga AW, Charles AC. Distinct vascular conduction with cortical spreading depression. *J Neurophysiol* 2007; **97**: 4143–4151.
32 Chuquet J, Hollender L, Nimchinsky EA. High-resolution *in vivo* imaging of the neurovascular unit during spreading depression. *J Neurosci* 2007; **27**: 4036–4044.
33 Takano T, Tian G, Peng W, Lou N, Lovatt D, Hansen AJ *et al.* Cortical spreading depression causes and coincides with tissue hypoxia. *Nat Neurosci* 2007; **10**: 754–762.
34 Sukhotinsky I, Dilekoz E, Moskowitz MA, Ayata C. Hypoxia and hypotension transform the blood flow response to cortical spreading depression from hyperemia into hypoperfusion in the rat. *J Cereb Blood Flow Metab* 2008; **28**: 1369–1376.
35 Peppiatt CM, Howarth C, Mobbs P, Attwell D. Bidirectional control of CNS capillary diameter by pericytes. *Nature* 2006; **443**: 700–704.
36 Yemisci M, Gursoy-Ozdemir Y, Vural A, Can A, Topalkara K, Dalkara T. Pericyte contraction induced by oxidative-nitrative stress impairs capillary reflow despite successful opening of an occluded cerebral artery. *Nat Med* 2009; **15**: 1031–1037.
37 Dreier JP, Major S, Manning A, Woitzik J, Drenckhahn C, Steinbrink J *et al.* Cortical spreading ischaemia is a novel process involved in ischaemic damage in patients with aneurysmal subarachnoid haemorrhage. *Brain* 2009; **132**: 1866–1881.
38 Dreier JP. The role of spreading depression, spreading depolarization and spreading ischemia in neurological disease. *Nat Med* 2011; **17**: 439–447.
39 Dreier JP, Körner K, Ebert N, Görner A, Rubin I, Back T *et al.* Nitric oxide scavenging by hemoglobin or nitric oxide synthase inhibition by N-nitro-L-arginine induces cortical spreading ischemia when $K+$ is increased in the subarachnoid space. *J Cereb Blood Flow Metab* 1998; **18**: 978–990.
40 Kader A, Frazzini VI, Solomon RA, Trifiletti RR. Nitric oxide production during focal cerebral ischemia in rats. *Stroke* 1993; **24**: 1709–1716.
41 Back T, Kohno K, Hossmann KA. Cortical negative DC deflections following middle cerebral artery occlusion and KCl-induced spreading depression: effect on blood flow, tissue oxygenation, and electroencephalogram. *J Cereb Blood Flow Metab* 1994; **14**: 12–19.
42 Takano K, Latour LL, Formato JE, Carano RA, Helmer KG, Hasegawa Y *et al.* The role of spreading depression in focal ischemia evaluated by diffusion mapping. *Ann Neurol* 1996; **39**: 308–318.
43 Hartings JA, Bullock MR, Okonkwo DO, Murray LS, Murray GD, Fabricius M *et al.* Spreading depolarisations and outcome after traumatic brain injury: a prospective observational study. *Lancet Neurol* 2011; **10**: 1058–1064.
44 Takagaki M, Feuerstein D, Kumagai T, Gramer M, Yoshimine T, Graf R. Isoflurane suppresses cortical spreading depolarizations compared to propofol - Implications for sedation of neurocritical care patients. *Exp Neurol* 2014; **252**: 12–17.

Supplementary Information accompanies the paper on the Journal of Cerebral Blood Flow & Metabolism website (http://www.nature.com/jcbfm)